JOURNAL OF APPLIED ELECTROCHEMISTRY **27** (1997) 379–384

Modelling the startup of a continuous parallel plate electrochemical reactor

J. M. BISANG

Programa de Electroquímica Aplicada e Ingeniería Electroquímica (PRELINE), Facultad de Ingeniería Química (UNL), Santiago del Estero 2829, 3000 Santa Fe, Argentina

Received 2 July 1996; revised 14 September 1996

A mathematical model to represent the startup operation of a continuous parallel plate electrochemical reactor is proposed. The model takes into account the diffusion layer adjacent to the working electrode and the convective region in the solution bulk. Experimental results of copper electrowinning from dilute solutions are compared with theoretical predictions. At short times the results are in close agreement with the transient equation derived from the diffusion layer and at larger times with that from the convective region. The mass transfer performance of the reactor is also analysed.

List of symbols

a_e	specific surface area (m^{-1})
A	electrode surface area (m^2)
C	concentration (mol m^{-3})
C_i	inlet concentration (mol m^{-3})
D	diffusion coefficient (m^2 s^{-1})
F	Faraday constant (A s mol^{-1})
H	Heaviside shifting function
i	current density (A m^{-2})
I	total current (A)
k	mass transfer coefficient (m s^{-1})
L	electrode length (m)
Q	volumetric flow rate (m^3 s^{-1})
S	interelectrode gap (m)
t	time (s)
t_0	time constant defined by Equation 8 (s)
v	superficial liquid flow velocity (m s^{-1})
W	electrode width (m)
x	coordinate (m)
y	coordinate (m)

Greek characters

δ	diffusion layer thickness (m)
ε	porosity
ν	kinematic viscosity (m^2 s^{-1})
ν_e	charge number of the electrode reaction
ρ	density (kg m^{-3})
σ	function defined by Equation 7
τ	reactor residence time (s)

1. Introduction

A detailed understanding of the time-varying behaviour of electrochemical reactors produced by perturbations in the inlet conditions or during the startup and shutdown operations is necessary in order to determine the transition time and to know the variations in the outlet conditions. Likewise, if the working conditions during the transition time are very different from the steady state values the characteristics and life time of the electrodes and separators can be affected and consequently the reactor performance can be altered.

Fahidy has studied the dynamic behaviour under perturbations in inlet conditions. In [1] the behaviour of isothermal electrochemical reactors according to the stirred tank and plug flow models is analysed when perturbations in the inlet concentrations and current are produced. In [2] the transient response of a nonisothermal continuous stirred tank electrochemical reactor is presented and in [3] the case of nonisothermal plug flow reactor is treated. In [4] the transient behaviour of an isothermal electrolyser consisting of a perfectly mixed-flow compartment and a batch compartment separated by an ion-selective membrane is analysed. In [5] the effect of flow-rate perturbations on the dynamics of tank flow electrolysers for the cases of: single flow electrolyser, the batch electrolyser with recycle, and the electrolyser cascade is analysed. In [6] an analysis of random perturbations in current and inlet electrolyte concentration is presented. Likewise, Scott [7] additionally examined the linearization of the perturbation equations for an isothermal continuous stirred tank reactor with input variations in flow-rate, concentrations and current density. Kreysa [8] also analysed concentration transients of idealized electrochemical reactors.

In contrast to this extensive literature concerning the dynamic behaviour under perturbations in inlet conditions, there is a scarcity of published work relevant to the start up of electrochemical reactors. Kreysa [8] analysed the start up and shut down in a stirred tank reactor. Rousar [9] calculated the time

0021-891X

necessary to attain a stationary diffusion and the theoretical results are compared to experimental data.

This work deals with the modelling of the start up operation of a parallel plate electrochemical reactor. The mathematical model considers the diffusion layer near the working electrode and a convective region in the solution bulk. The theoretical predictions are compared with experimental results.

2. Mathematical model

A rigorous treatment of the startup of a continuous parallel plate electrochemical reactor requires the solution of the time-dependent convective diffusion equation with appropriate hydrodynamic relations. However, in order to avoid the mathematical complexity and to obtain an analytical expression for the transient behaviour a simplified model is proposed. The main assumption of the model is to consider the solution phase formed by two zones: a thin boundary layer of thickness δ at the working electrode and a convective region. The boundary layer is assumed stagnant and the mass transfer in it is by diffusion. Likewise, in the boundary layer longitudinal gradients of concentration are considered negligible compared to transverse gradients (y coordinate). Although in the convective region a flat profile of velocity is assumed, the mass transfer is by convection and the variation of concentration is considered only in the longitudinal direction. Figure 1 shows a schematic view of the model. Further simplifying assumptions of the model are: (a) the metal phase of the electrodes is isopotential; (b) the reactor is isothermal; (c) the hydrodynamics is in steady state before the current is connected; (d) the entrance effects are ignored; and (e) at the working electrode a mass-transfer controlled reaction takes place and the reaction at the counter electrode is governed by charge transfer. This situation represents the electrowinning of metals.

The concentration variation in the diffusion layer is given by Fick's second law

$$\frac{\partial C(y,t)}{\partial t} = D\frac{\partial^2 C(y,t)}{\partial y^2} \tag{1}$$

with the initial and boundary conditions:

$$t = 0 \qquad C = C_i \qquad \text{for all } y \tag{1a}$$

$$y = 0 \qquad C = 0 \qquad \text{for } t > 0 \tag{1b}$$

$$y = \delta \qquad C = C(x,t) \tag{1c}$$

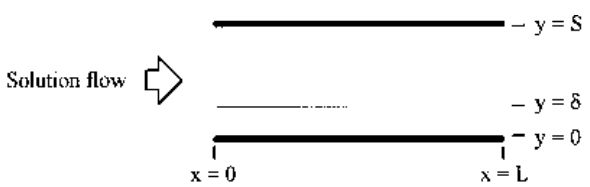

Fig. 1. Schematic view of the parallel plate electrochemical reactor and coordinates.

Condition 1(a) expresses the homogeneity of the solution before the current is connected. According to the Condition 1(b), the applied potential to the working electrode is sufficiently negative to achieve a zero concentration at the electrode surface. Therefore, the reaction rate is controlled by diffusion of the electroactive substance. Condition 1(c) expresses that, for a given x value, the concentration is uniform for y values higher than δ.

The current density is given by

$$i(x,t)|_{y=0} = v_e FD\left.\frac{\partial C(y,t)}{\partial y}\right|_{y=0} \tag{2}$$

In the convective region, plug flow is assumed. The mass balance gives

$$\varepsilon\frac{\partial C(x,t)}{\partial t} = -v\frac{\partial C(x,t)}{\partial x} - \frac{i(x,t)|_{y=\delta} a_e}{v_e F} \tag{3}$$

with the following initial and boundary conditions:

$$t = 0 \qquad C = C_i \qquad \text{for all } x \tag{3a}$$

$$x = 0 \qquad C = C_i \qquad \text{for all } t \tag{3b}$$

Due to the small value of δ the normal component of the current density is assumed constant in the boundary layer at a given position along the cell, that is,

$$i(x,t)|_{y=0} = i(x,t)|_{y=\delta} \tag{4}$$

The total current, for the reactor, is given by

$$I(t) = W\int_0^L i(x,t)\mathrm{d}x \tag{5}$$

Therefore, when in an electrochemical reactor with steady state solution flow the current is connected, two processes take place. A concentration profile is built up in the y direction inside the boundary layer and a concentration profile is simultaneously generated in the convective region along the reactor. The consecutive solution of Equations 1 to 5 yields the current as a function of time.

Cottrell [10] obtained the solution of the boundary layer problem, Equations 1 and 2:

$$i(x,t)|_{y=0} = v_e FkC(x,t)[1+\sigma(t)] \tag{6}$$

where

$$\sigma(t) = 2\sum_{m=1}^{\infty}\exp\left(-m^2\frac{t}{t_0}\right) \tag{7}$$

with

$$t_0 = \frac{\delta^2}{\pi^2 D} \tag{8}$$

Combining Equations 3, 4 and 6 results

$$\varepsilon\frac{\partial C(x,t)}{\partial t} = -v\frac{\partial C(x,t)}{\partial x} - ka_e C(x,t)[1+\sigma(t)] \tag{9}$$

Vetter [11] demonstrated that for $t > 3t_0$ the current density $i(t)$ is higher than the steady-state value by only 10%. Taking into account that in the usual

systems the t_0 values are very small and in order to simplify the mathematical treatment $\sigma(t)$ can be neglected. Therefore, Equation 9 is simplified to

$$\varepsilon\frac{\partial C(x,t)}{\partial t} = -v\frac{\partial C(x,t)}{\partial x} - ka_e C(x,t) \qquad (10)$$

valid when the concentration profile in the diffusion layer is established. By Laplace transforms the solution of Equation 10 is

$$C(x,t) = C_i\left\{\exp\left(-\frac{ka_e t}{\varepsilon}\right) + \left\{1-\exp\left[-\frac{ka_e}{\varepsilon}\left(t-\frac{x\varepsilon}{v}\right)\right]\right\} \exp\left(-\frac{ka_e x}{v}\right) H\left(t-\frac{x\varepsilon}{v}\right)\right\} \qquad (11)$$

with

$$H\left(t-\frac{x\varepsilon}{v}\right) = 0 \qquad t < \frac{x\varepsilon}{v} \qquad (11a)$$

$$H\left(t-\frac{x\varepsilon}{v}\right) = 1 \qquad t \geq \frac{x\varepsilon}{v} \qquad (11b)$$

For $t \geq x\varepsilon/v$ the steady-state concentration is obtained:

$$C(x) = C_i \exp\left(-\frac{ka_e x}{v}\right) \qquad (12)$$

According to Equation 11 the connection of the current is felt immediately at each point of the reactor up to time instant $x\varepsilon/v$. Therefore, taking into account only the convective region the time necessary to reach the steady state is $L\varepsilon/v$, the reactor residence time.

Combining Equations 11, 11(a) and (b), and 5 gives

$$I(t) = Wv_e FC_i\left\{\int_0^L \exp\left(-\frac{ka_e t}{\varepsilon}\right)dx + \int_0^{tv/\varepsilon}\left\{1-\exp\left[-\frac{ka_e}{\varepsilon}\left(t-\frac{x\varepsilon}{v}\right)\right]\right\} \exp\left(-\frac{ka_e x}{v}\right)dx\right\} \qquad (13)$$

Solving Equation 13 and rearranging

$$I(t) = Qv_e FC_i\left[1-\exp\left(-\frac{ka_e t}{\varepsilon}\right) + \frac{ka_e}{\varepsilon}\exp\left(-\frac{ka_e t}{\varepsilon}\right)(\tau - t)\right] \qquad (14)$$

Equation 14 presents the following limiting values

$$I(0) = v_e FkAC_i \qquad (15)$$

and

$$I(\tau) = Qv_e FC_i\left[1-\exp\left(-\frac{ka_e L}{v}\right)\right] \qquad (16)$$

which is the mass balance in steady state.

Therefore, the dynamic behaviour of the electrochemical reactor can be represented by two equations. At short times after the connection the current is given by Equation 6 evaluated at the inlet concentration and multiplied by the electrode surface area and at higher times, when the boundary layer has achieved the steady state, Equations 14 is valid.

3. Experimental details

Figure 2 shows a general diagram of the experimental setup. All experiments were performed in an electrochemical reactor with vertical parallel plate electrodes. The reactor was made of acrylic material and both electrodes had the same dimensions, 200 mm wide and 600 mm long. To increase the mass transfer coefficient and to make it independent of the position in the reactor, the interelectrode gap, 13 mm, was completely filled with 16 sheets of plastic net, 0.4 mm thread diameter and 1.29 mm × 1.55 mm mesh size. The porosity of the stacked nets was 0.82. The small value of the aspect ratio (i.e., the ratio of electrode separation to electrode length) justifies the use of the plug-flow model for the convective region. The anode was a sheet of expanded titanium, 0.75 mm thick, coated with RuO_2. Nickel coated with copper was used as cathode.

All experiments were performed under potentiostatic control. The potential of the working electrode was –0.4 V against the saturated calomel electrode. This potential value was determined in a further experiment with a rotating disc electrode, where it was observed that at –0.4 V the reaction is under limiting current condition and the hydrogen evolution is hindered.

The solution flowed from a thermostated tank (30 °C) to the lower part of the reactor, and was collected in another tank. It was not recycled in order that the inlet copper concentration remained constant. The flow circuit system also included a rota-

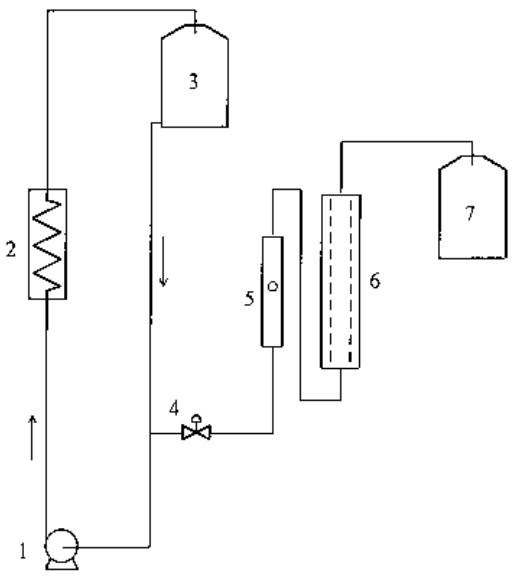

Fig. 2. Scheme of the electrolyte circulation system: (1) pump; (2) thermostat; (3) thermostated tank; (4) needle valve; (5) flowmeter; (6) reactor; (7) reservoir.

Table 1. Physical properties of the solution at 30 °C

Property	*Value*
Kinematic viscosity, ν	1.11×10^{-6} m^2 s^{-1}
Density, ρ	1.11×10^{3} kg m^{-3}
Diffusion coefficient, D	5.16×10^{-10} m^2 s^{-1}
Schmidt number, Sc	2151

meter and a needle valve. The solution flow in the reactor was upwards and in order to achieve more uniform flow conditions along it, flow distributor plates with numerous small holes were arranged in the inlet and outlet regions. The same flow distributors were previously used [12] in a reactor with segmented counter electrode without plastic nets in the interelectrode gap and entrance effects were observed only in the first segment, approximately 2.5 cm. Likewise, Brown *et al.* [13] used plastic mesh promoters to help to reduce entrance effects near the inlet manifold. Therefore, in the present reactor the entrance length is negligible compared to the total electrode length.

The electrolyte solution was 1 M Na_2SO_4 and H_2SO_4, to obtain pH 2, with a copper concentration of approximately 1 g l^{-1}. The physical properties of the solution are given in Table 1. Therefore, the anodic reaction was oxygen evolution and copper deposition was the cathodic reaction. For each experiment the copper concentration was determined by iodimetry [14] with an accuracy of 0.7%.

4. Results and discussion

Prior to the dynamic behaviour studies the mass transfer performance of the electrochemical reactor was analysed. The volumetric mass transfer coefficients were calculated using Equation 16. Figure 3 shows the ka_e values as a function of velocity referred to the empty cross section of the reactor. The correlation of the experimental results yields

$$ka_e = 4.75 \times 10^{-3} v^{0.55} \qquad (17)$$

with a linear correlation coefficient of 0.99. The units of ka_e are s^{-1} and those of v are m s^{-1}. In Equation 17 the exponent of the velocity is close to values previously reported [15, 16].

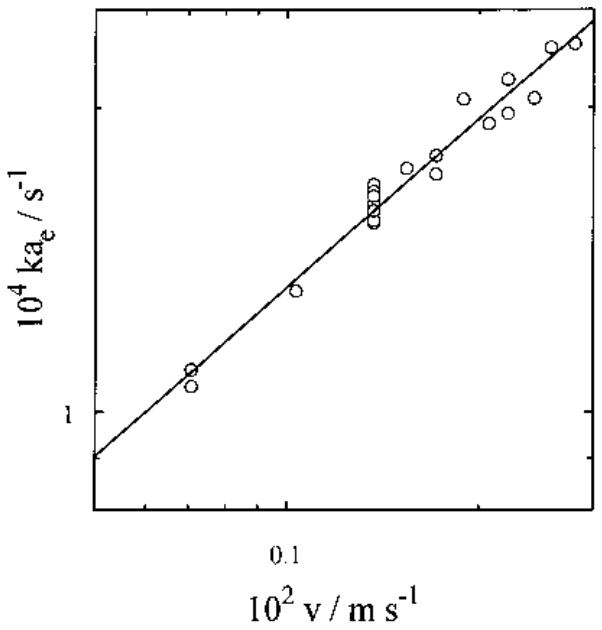

Fig. 3. Variation of ka_e with the superficial liquid flow velocity.

Table 2 summarises the experimental results. It can be observed that the t_0 values are lower than 4% of the reactor residence time. Therefore, the neglecting of $\sigma(t)$ in Equation 9 is justified.

Figure 4 shows the current as a function of time for different solution flow rates. The full lines represent the experimental results. The dashed lines correspond to Equation 6 evaluated at the inlet concentration and multiplied by the electrode surface area and the dotted lines to Equation 14. The residence time is indicated in each figure. It can be observed that at short times there is a close agreement between the experimental results and Equation 6. Analogously, Equation 14 agrees satisfactorily with the experimental data at larger times. Unfortunately, in the middle range of times both theoretical equations predict currents lower than the experimental ones. Likewise, the results of Equation 9 without the rejection of $\sigma(t)$ will lie between those of Equations 6 and 14 and a more exact prediction of the experimental data is not achieved.

Analysing both theoretical curves it is concluded that the times to achieve a steady state corresponding to the boundary layer are shorter than those required

Table 2. Summary of the experimental results

$10^3\ v$ / m s^{-1}	τ / s	$10^6\ k$ / m s^{-1}	$10^4\ \delta$ / m	t_0 / s	t_0/τ / %
0.0805	6114.84	0.764	6.75	89.47	1.46
0.389	1264.46	1.02	5.06	50.27	3.98
0.707	695.70	1.38	3.74	27.47	3.95
1.04	475.36	1.71	3.02	17.91	3.77
1.37	358.86	2.00	2.58	13.07	3.64
1.72	286.55	2.23	2.31	10.48	3.66
2.07	237.34	2.50	2.06	8.33	3.51
2.44	201.81	2.65	1.95	7.47	3.70
2.81	174.96	3.01	1.71	5.74	3.28

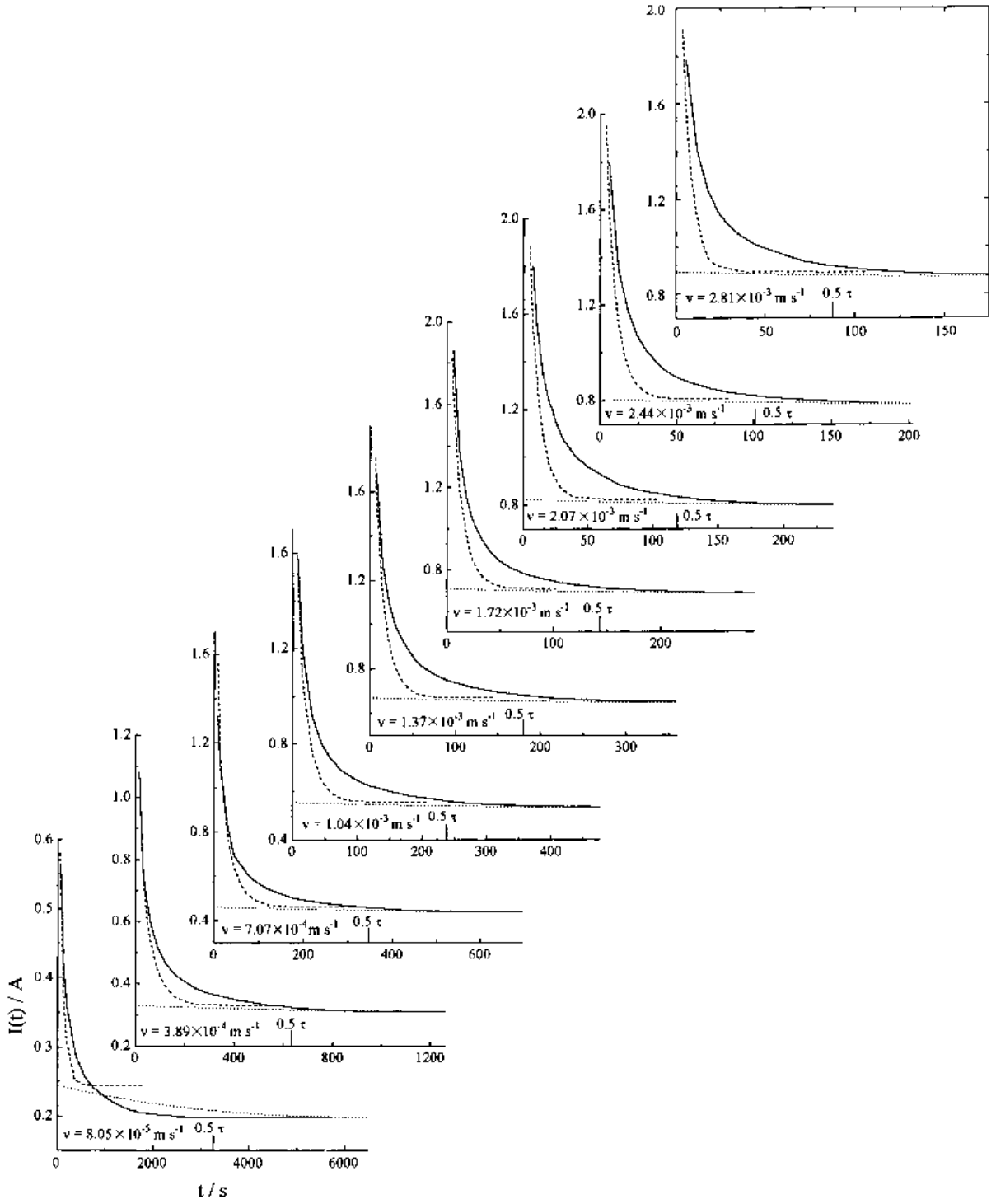

Fig. 4. Current as a function of time at different superficial liquid flow velocities. Full lines: experimental results. Dashed lines: Equation 6 evaluated at the inlet concentration and multiplied by the electrode surface area. Dotted lines: Equation 14.

by the convective region. This justifies the mathematical solution of Equation 9 without considering $\sigma(t)$.

Comparing the different curves of Figure 4 it can be observed that flow rate increases decrease the prediction capability of Equation 6. For the highest value of the solution flow rate the experimental current is between 10–20 % higher than the theoretical one. This conclusion agrees with previous studies [9]

References

[1] T. Z. Fahidy, 'Principles of Electrochemical Reactor Analysis', Elsevier, Amsterdam (1985), chapter 10, p. 244.
[2] T. Z. Fahidy, *J. Appl. Electrochem.* **14** (1984) 231.
[3] *Idem, Electrochim. Acta* **29** (1984) 1321.
[4] *Idem, J. Appl. Electrochem.* **18** (1988) 104.
[5] *Idem, J. Electrochem. Soc.* **136** (1989) 2552.
[6] *Idem, J. Appl. Electrochem.* **20** (1990) 901.
[7] K. Scott, 'Electrochemical Reaction Engineering', Academic Press, London (1991), chapter 5, p. 310.

[8] G. Kreysa, *DECHEMA Monogr.* **120** (1989) 107.
[9] I. Rousar, K. Micka and A. Kimla, 'Electrochemical Engineering I', Elsevier, Amsterdam (1986), chapter 19, p. 314.
[10] F. G. Cotrell, *Z. Phys. Chem.* **42** (1903) 385.
[11] K. J. Vetter, 'Electrochemical Kinetics. Theoretical and Experimental Aspects', Academic Press, New York (1967), chapter 2, p. 218
[12] J. M. Bisang, *J. Appl. Electrochem.* **23** (1993) 966.
[13] C. J. Brown, D. Pletcher, F. C. Walsh, J. K. Hammond and D. Robinson, *ibid.* **22** (1992) 618.
[14] W. Rieman and J. D. Neuss, 'Quantitative Analysis', McGraw Hill, New York (1937), chapter XV, p. 184.
[15] P. M. Robertson, F. Schwager and N. Ibl, *J. Electroanal. Chem.* **65** (1975) 883.
[16] F. Goodridge and K. Scott, 'Electrochemical Process Engineering', Plenum Press, New York (1995), chapter 2, p. 44.